

iScience, Volume 25

Supplemental information

**Glycosylation network mapping and site-specific
glycan maturation *in vivo***

Marie-Estelle Losfeld, Ernesto Scibona, Chia-wei Lin, and Markus Aebi

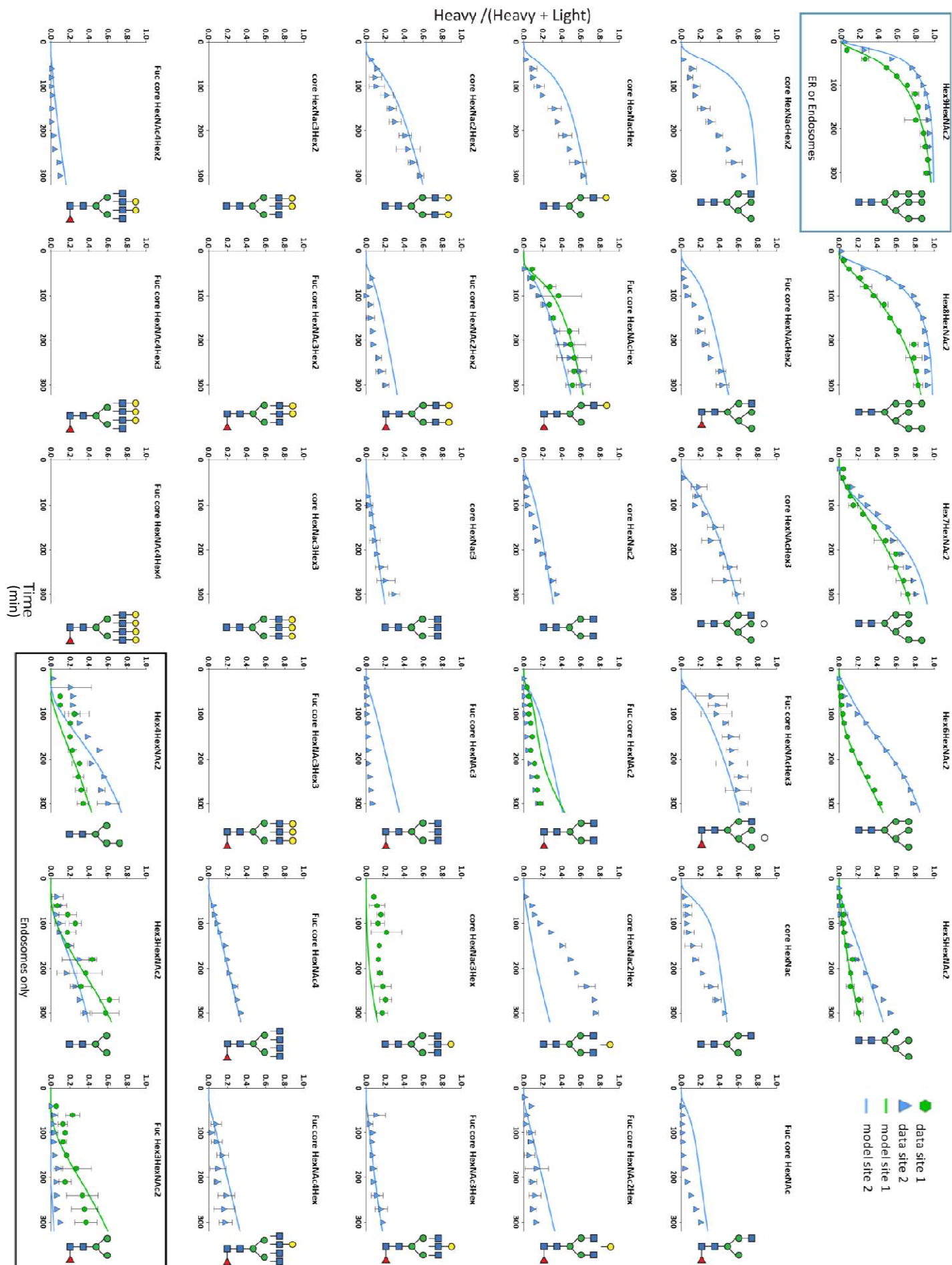
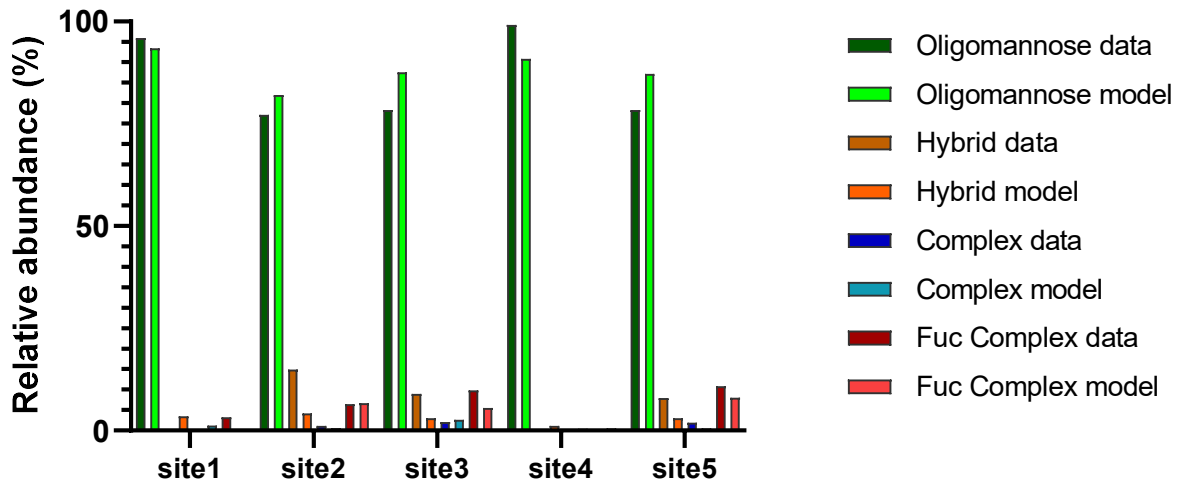
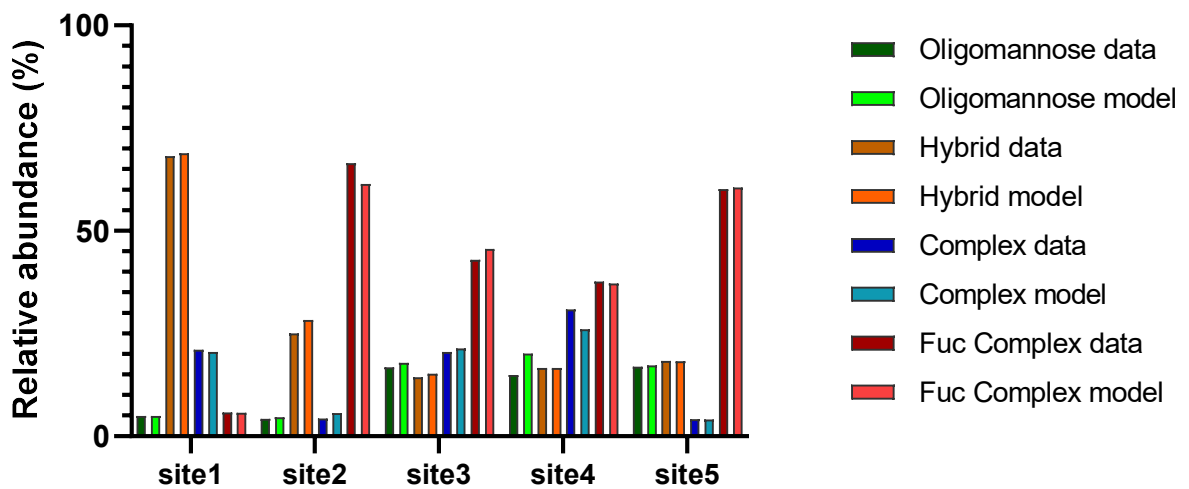


FIGURE S1: SITE-SPECIFIC INTRACELLULAR GLYCAN TURNSOVERS AND MODELED KINETICS OF SITE 1 AND 2 Related to Figure 2

The site-specific glycan turnovers are represented by the plotting of the fractional labeling (heavy signal / (heavy + light)) of each glycan intermediates over time. A representation of the glycan structure was added on the left of its corresponding plot, potential isoforms are not represented. The different sites are represented by shapes color coded as follows: site1 in green, site2 in blue. The modeled turnover kinetics are shown as solid line curves of the corresponding colors. Each data point represents the average of three biological replicates. Error bars represent the calculated standard deviations.

A**Intracellular abundance****B****Secreted abundance****FIGURE S2: RELATIVE ABUNDANCE PREDICTION ACCURACY BY THE MODEL** Related to Figure 1 and 5

- A. Comparison of the relative intracellular abundance of the different glycan types as calculated by the model with the biological data. The structures were grouped in four glycan types: oligomannose, hybrid, complex and fucosylated complex.
- B. Comparison of the relative secreted abundance of the different glycan types as calculated by the model with the biological data. The structures were grouped in four glycan types: oligomannose, hybrid, complex and fucosylated complex.

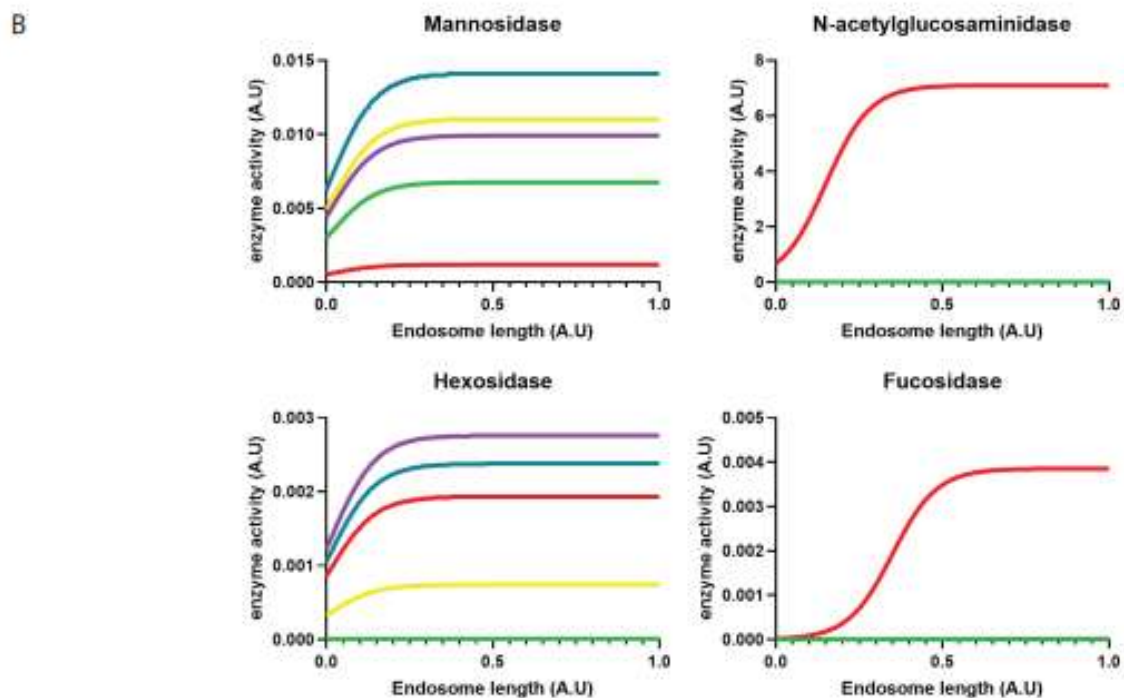
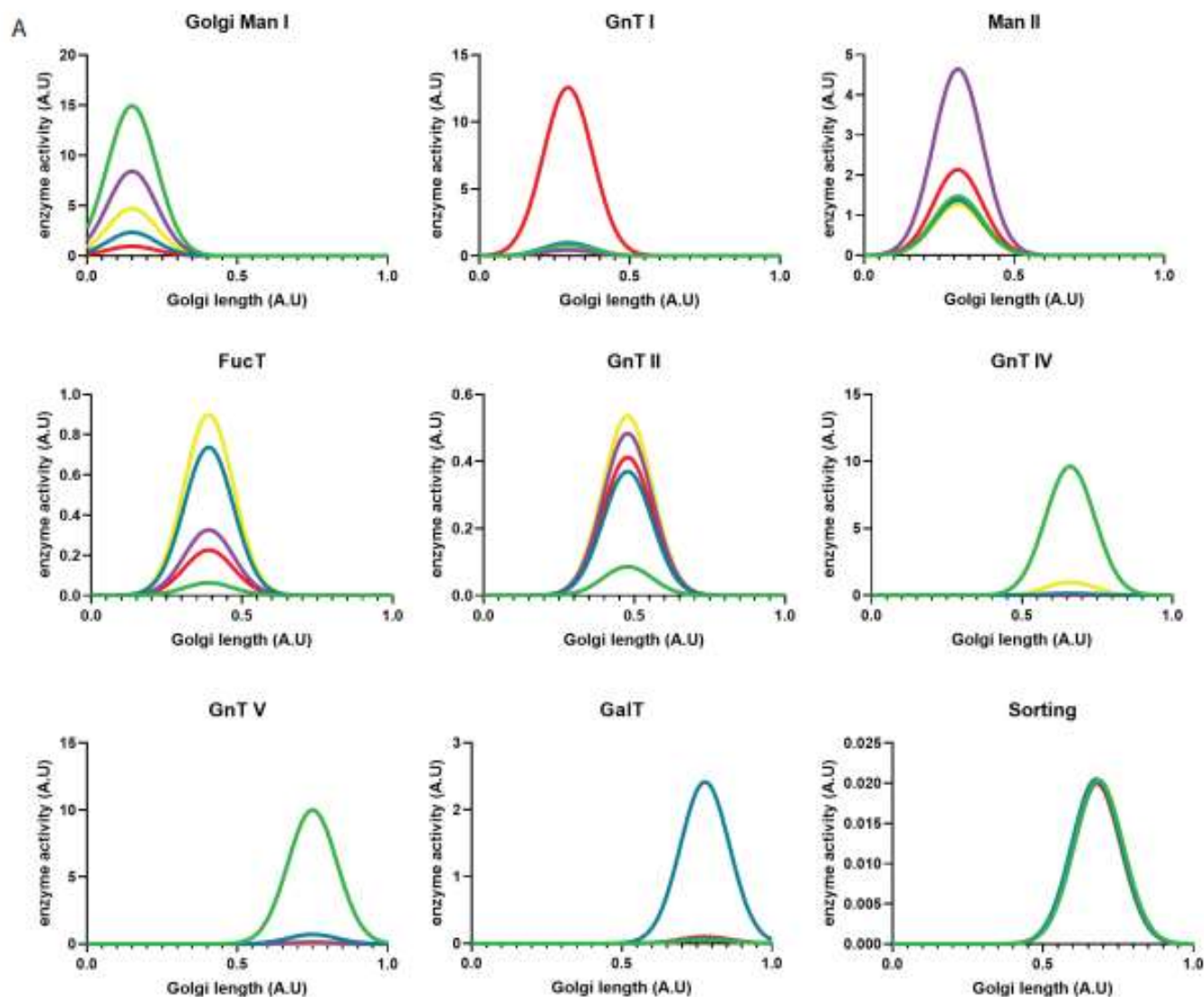


FIGURE S3: ENZYMATIC ACTIVITY PER SITE Related to Figure 5

A. Site-specific Golgi enzymatic activity. The activity of each Golgi enzyme relative to each Pdi's glycosite (in arbitrary units) was plotted separately in function of the Golgi length

B. Site-specific hydrolases activity in the endosomes. The activity of each hydrolase relative to each Pdi's glycosite (in arbitrary units) was plotted separately in function of the endosome length.

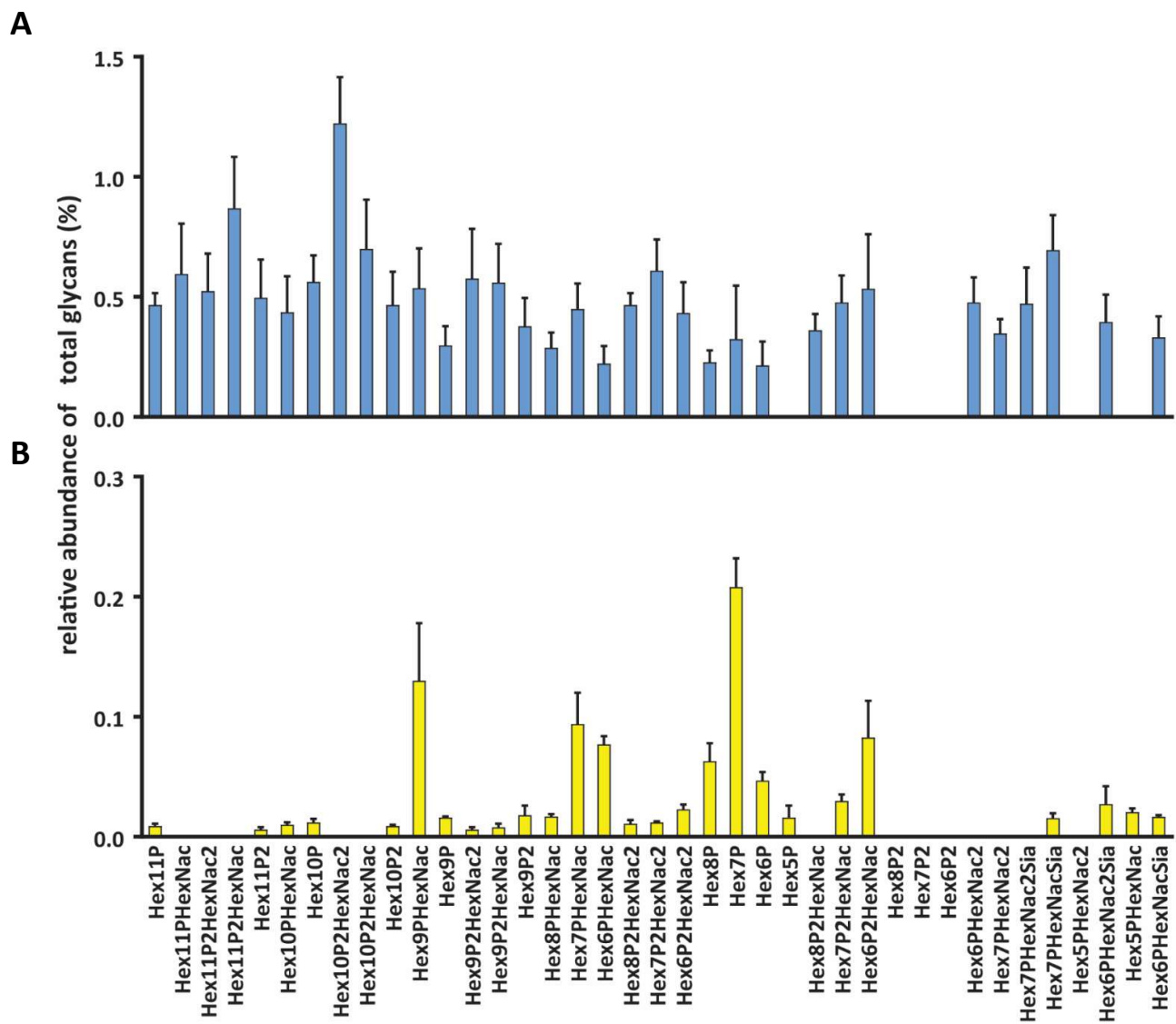


FIGURE S4: INTRACELLULAR RELATIVE ABUNDANCE OF PHOSPHORYLATED GLYCANS Related to Figure 7

Panel A and B represent respectively the relative abundance of the phosphorylated glycans on a site 2 and site 5. Data represent the average of three biological replicates. Error bars represent the calculated standard deviations.

A

Variable Name	Unit	Value_PDI
k_Transport_ER_Lys	-	1.36E-02
k_deg_Lys	-	2.98E-03
k_folding	-	9.03E-03
E _{max} _Sorting	-	4.05E-02
z_Sorting	-	6.81E-01
t_Endo	min	8.50E+02
t_Golgi	min	2.00E+01
z_Mani	-	1.50E-01
z_GnT I	-	2.95E-01
z_Man II	-	3.13E-01
z_FucT	-	3.90E-01
z_GnT II	-	4.78E-01
z_GnT III	-	6.60E-01
z_GnT IV	-	7.50E-01
z_GalT	-	7.77E-01
z_Hexosidases_Endo	-	1.50E-02
z_Fucosidase_Endo	-	3.50E-01
z_Hexosaminidase_Endo	-	1.50E-01
w_gaussian_Golgi	-	8.16E-02

B

Variable Name	Value Site1	Value Site2	Value Site3	Value Site4	Value Site5
k_Glc3A -> k_Glc2A	5.97E-01	5.84E+02	1.00E+03	6.35E-01	3.08E+01
k_Glc2A -> k_Glc1A	1.00E+03	1.15E+02	7.60E+02	5.51E+02	1.00E+03
k_Glc1A -> k_Man9	3.97E+01	1.00E+03	5.14E+02	8.86E+02	6.96E+02
k_Glc3B -> k_Glc2B	5.48E-03	1.95E-02	3.03E-03	1.00E-03	3.30E-03
k_Glc2B -> k_Glc1B	4.83E+02	1.00E-03	7.50E+00	1.00E-03	1.08E+01
k_Glc1B -> k_Man9	3.26E-01	1.00E-03	6.79E+00	2.19E+01	9.00E+01
kMan 9->Man8 (ER)	2.31E-02	8.90E-02	6.85E-02	3.81E-02	4.59E-02
kMan 8->Man7 (ER)	2.50E-02	2.57E-02	2.64E-02	3.15E-01	2.22E-02
k Man7->Man6 (ER)	9.20E-03	5.52E+00	2.01E-05	8.27E-01	3.76E-03
k Man6->Man5 (ER)	7.52E-01	2.39E-01	3.61E-01	9.81E-01	1.42E+00
k Man5->Man4 (ER)	3.26E-03	8.14E-03	5.07E-03	7.75E-01	1.26E+00
k Man4->Man3 (ER)	5.74E+00	4.47E+00	8.35E-01	7.20E-01	5.60E-03
k Man3->Man2 (ER)	8.13E-01	7.61E+00	1.16E+00	7.21E+00	2.05E-01
Mani_Max_Activity	2.99E+01	4.70E+00	1.69E+01	1.93E+00	9.44E+00
GnT I_Max_Activity	1.63E+00	1.97E+00	8.80E-01	2.51E+01	9.07E-01
Man II_Max_Activity	2.94E+00	2.75E+00	9.29E+00	4.27E+00	2.54E+00
FucT_Max_Activity	1.27E-01	1.47E+00	6.52E-01	4.51E-01	1.80E+00
GnT II_Max_Activity	1.73E-01	7.40E-01	9.67E-01	8.25E-01	1.07E+00
GnT III_Max_Activity	1.92E+01	1.91E-01	2.89E-01	2.85E-02	1.97E+00
GnT IV_Max_Activity	2.00E+01	1.43E+00	2.77E-01	1.84E-01	2.01E-02
GalT_Max_Activity	1.08E-01	4.83E+00	1.78E-01	1.94E-01	2.23E-01
Mannosidase_Endo_Max_Activity	6.76E-03	1.41E-02	9.92E-03	1.19E-03	1.10E-02
Hexosaminidase_Endo_Max_Activity	1.43E-02	6.69E-04	3.60E-04	7.10E+00	5.50E-05
Fucosidase_Endo_Max_Activity	1.00E-06	1.47E-06	8.46E-06	3.85E-03	1.12E-06
Hexosidase_Endo_Max_Activity	1.00E-05	2.38E-03	2.76E-03	1.93E-03	7.43E-04

TABLE S3: Related to Figure 4

A. Protein specific kinetic parameters calculated by the mathematical model for enzymatic and transport events. k = kinetic constant, z = position, w = width gaussian distribution, E_{max} = peak activity for enzyme

B. Site-specific kinetic parameters calculated by the mathematical model for specific enzymatic and transport events